Seismological Institute
The University
Uppsala, Sweden

Uppsala, Jan. 15, 1964

European Office
Office of Aerospace Research
Shell Building
47 Cantersteen
Brussels, Belgium

AD665404

Fourth Semi-Annual Technical Report

(Report No. 23)

Period Covered: July 1 - December 31, 1963

ARPA Order No. 180-62,	Amendment No. 7, dated 3 Aug. 1961
Project Code Number:	8100
Name of Contractor:	University of Uppsala Uppsala, Sweden
Date of Contract:	1 May 1962
Contract Number:	AF 61(052)-588
Amount of Contract:	$ 19,120.00
Contract Expiration Date:	30 June 1963
Name and Phone Number of Project Scientist:	Dr. Markus Båth Seismological Institute 130258
Short Title of the Work:	Rheologic Properties of the Solid Earth.

The investigations reported in the Third Semi-Annual Technical Report (Report No. 16) have been continued and extended. Below, we describe the research done, according to the items listed in the contract:

1. Strain release studies.
2. Laboratory studies of scale models under stress.
3. Development of a method to measure stress variations in the crust.

In addition, the report contains the following two items:

4. S.J. Duda's visit to USA for study and research.
5. Bibliography.

Complete manuscripts of two papers are attached as Appendixes I and II.

All the research within this contract has been conducted by the following two persons:

Seweryn J. Duda, full-time

Markus Båth, part-time.

1. Strain release studies

a. Western part of the North American Continent

Our strain release studies are concerned with the ciroum-Pacific earthquake belt. The purpose is mainly to investigate possible mutual dependences of seismic activity in adjacent areas. Earlier, three sequences in California (Kern County 1952, Desert Hot Springs 1948, San Francisco 1957) and the Chile earthquakes 1960 were investigated. See 1. and 2. in the Bibliography. In this period, the western part of the North American Continent was included in these investigations.

First, the seismicity of West Canada for the interval 1955-1959 was investigated. In the formula $\log N = a - bM$, where N is the number of shocks in the magnitude range $M \pm 0.05$, we found that the coefficient $b = 0.58$ for $M \geq 2.4$. This is a relatively low value of b. One of the main difficulties in investigations of this type is to limit off the observational material correctly in space and time. In this case, we gradually found it necessary to extend the observations to cover the whole of western North America between latitudes 10°N and $67\frac{1}{2}^{\circ}$N and to extend them in time to cover the 11-year interval 1949-1959. Our listed material is most probably complete for earthquakes with $M \geq 6.0$. A time-space diagram has been constructed, like the one earlier made for Chile (see 2.). We are still working on the search for possible migration patterns. More elaborate statistical technique will be used in order to ascertain the significance of any migration patterns found. Although there are some indications of migration, there is so far no reliable proof of their existence in this case.

b. Non-Alpide Asia

We have extended our strain release studies to include also one or two aftershock sequences from the continental, non-Alpide Asia, mainly to get observational material from an area which, according to some indications, exhibits a pattern different from the Pacific belt. We have already begun with the Mongolian sequence, starting on December 4, 1957, and have tentatively planned to include a sequence in China (Chinghai Province,

May 21, 1962).

The investigation of the Mongolian sequence from 1957 has so far yielded the following results. All earthquakes with magnitude $M \geq 5.2$ have been listed for 3½ years following the main shock. The b-coefficient in the formula $\log N = a - bM$ was found to be 0.7 for this material, i.e. about the same as for Chile (see 2.). A strain release characteristic has been constructed, which exhibits two branches. These can be approximated by a logarithmic and an exponential curve resp. However, these curves will be reconstructed in the light of new findings (see 1.d. below). In the first stage of the sequence, the epicenters of the aftershocks were distributed along an E-W striking fault. On December 3, 1960, some seismic activity started on an adjacent fault, extending toward SE from the eastern end of the old fault, under an angle of 40° with this fault. The activity on the second fault is most likely caused by the pre-existing activity on the first fault. Our photoelastic experiments have indeed provided an explanation for this behaviour (see 2. below).

In order to study possible changes of focal mechanism during the aftershock sequence, as the case was with Kern County 1952, records have been collected from many stations for a few of the aftershocks.

c. Other aftershock sequences

There are quite a number of other aftershock sequences, which deserve to be investigated. Among these might be mentioned two Kurile Islands sequences, starting on Nov. 6, 1958, and Oct. 13, 1963, respectively. Such sequences will be included in the work under the present contract to the extent that time will permit and if they are likely to throw further light on our problems.

d. Improvement of the methods

Benioff initiated strain release studies around 1950. Since that time the same methods, as originally given by Benioff, have been used by all who have worked in this field, including ourselves. In the original method, strain is proportional to the square root of the released energy. The volume of every aftershock was considered constant and equal to the total volume

of the aftershock zone. Moreover, an older energy-magnitude formula has been used for consistency reasons, although newer and better formulas have been developed in the meantime. The fraction of elastic strain energy converted into seismic energy was also assumed constant. It occurred to us that time had come to improve Benioff's method in the light of new findings.

Under the assumption that the volume of an earthquake is defined by the total volume occupied by its aftershocks, it was possible to deduce a relation between earthquake volume and magnitude. The volume was found to increase with magnitude, at about the same rate as energy increases with magnitude. Strain was found to be independent of magnitude, within our error limits. Therefore, the difference between large and small shocks is mainly a difference in the volume and not in the strain, a result which may seem surprising but is in better accord with general inferences from rock behaviour under stress. As a consequence, some of our earlier strain release characteristics have been reconstructed, now as deformation characteristics instead.

A paper has been prepared for publication, and its complete manuscript is attached to the present report (Appendix I).

2. Laboratory studies of scale models under stress

Our laboratory studies aim at a duplication of natural stress phenomena by means of controlled experiments in which various parameters can be varied at will (both under static and, if possible, also under dynamic conditions). In the autumn of 1962, it occurred to us that the photoelastic method would be most suitable for this kind of work.

Photoelastic measurements require long experience in order to lead to meaningful results and a well-equipped photoelastic laboratory also means quite a lot of expenses. However, we were very fortunate in obtaining the expert advice of Dr. R. Hiltscher, Stockholm, who is a well-known authority on photoelasticity, also we had the fortunate possibility to work in the laboratory of the Royal Water Power Board ("Statens Vattenfallsverk") in Stockholm.

To date, the two-dimensional stress field has been determined in different plates: first in one with an open slit, then in a plate with a closed slit (zone of weakness) under two different angles to the direction of the applied pressure field. Part of the evaluation of the measurements was made on a digital computer of the Swedish Board for Computing Machinery, Stockholm. The preliminary investigations, so far carried out, are reported with all details in an attached paper (Appendix II). Some features of earthquake occurrences are explained in the light of our new findings from these experiments.

The steady stress state in a perfect elastic model can only give a partial analogy to real tectonic conditions, as the stress state in the orogenetic shell changes with time and the material in the orogenetic shell exhibits elastic afterworking. Later, we will try to construct models with time-dependent elastic properties and to investigate them by the photoelastic analogue processing.

3. Development of a method to measure stress variations in the crust

Direct measurements of stress in natural rock under a certain time interval in order to follow its variations with time are of great importance in connection with our studies. To our knowledge, the sond developed by Prof. N. Hast, Stockholm, provides one of the best possibilities for this kind of research. Prof. Hast originally developed his sond for stress measurements in concrete, but has in recent years applied it mainly to test rock stability in mines. He has collected a number of instantaneous point measurements, especially in the Fennoscandian area. His results are certainly of great geophysical interest.

The Fennoscandian area is very quiet from the seismic point of view, and what we could find from continuous stress measurements could be stress variations due to earth tides and to some other phenomena (variations of atmospheric pressure etc). Such measurements should be collocated with similar measurements in seismically active areas, especially in Japan,

where they would be of great importance also for the earthquake predicition program which is under way there. Prof. Hast has himself also tried to get UNESCO interested in supporting such measurements.

We have repeatedly been in contact with Prof. Hast, who always shows great interest for the geophysical applications of his method, but so far we have unfortunately not been able to activate him sufficiently to get some real collaboration started. At present, it seems to be questionable to what extent this will succeed during the remaining 18 months of the contract.

4. S.J. Duda's visit to USA for study and research

As originally planned, Mr. S.J. Duda will spend some time in USA to continue his study and research within the items of the contract. We have now planned that Duda will spend the first six months of 1964 in USA, mainly at the Seismological Laboratory, Pasadena, California, where he will continue his research under the guidance of Prof. H. Benioff. As already agreed, Duda will receive the travel expenses from the contract, and the cheapest possible air transportation will be used. As a partial compensation for the higher living costs in USA as compared to Sweden, I suggest that Duda's monthly payment be raised to 2500:- Sw. Cr. during his stay in USA, all within the contract.

5. Bibliography

This bibliography gives a complete list of papers produced up to now within this contract.

1. S.J. Duda & M. Båth: Strain release in the circum-Pacific belt: Kern County 1952, Desert Hot Springs 1948, San Francisco 1957, Geophys. Journ., Vol. 7, pp. 554-570, 1963.

2. S.J. Duda: Strain release in the circum-Pacific belt: Chile 1960, Journ. Geophys. Res., Vol. 68, pp. 5531-5544, 1963.

3. M. Båth & S.J. Duda: Strain release in relation to focal depth, Geofis. pura e appl., in press.

4. S.J. Duda & M. Båth: Earthquake volume, fault plane area, seismic energy, strain, deformation and related quantities, Appendix I to the present report, intended for publication in Ann. di Geofisica.

5. S.J. Duda: The stress field around a fault according to a photoelastic model experiment, Appendix II to the present report, intended for publication in Geophys. Journ.

Markus Båth

Markus Båth
Project Scientist

A P P E N D I X I

EARTHQUAKE VOLUME, FAULT PLANE AREA, SEISMIC ENERGY, STRAIN, DEFORMATION AND RELATED QUANTITIES

Markus Båth and Seweryn J. Duda

Seismological Institute

University of Uppsala

Uppsala, Sweden

Contract No. AF 61(052)-588

January 15, 1964

Prepared for

GEOPHYSICS RESEARCH DIRECTORATE

AIR FORCE CAMBRIDGE RESEARCH LABORATORIES

OFFICE OF AEROSPACE RESEARCH

UNITED STATES AIR FORCE

BEDFORD, MASSACHUSETTS

WORK SPONSORED BY ADVANCED RESEARCH PROJECTS AGENCY

PROJECT VELA-UNIFORM

ARPA Order No. 180-62, Amendment No. 7,

dated 3 Aug. 1961

Project Code No. 8100, Task 86520

Intended for publication in Annali di Geofisica, Rome

EARTHQUAKE VOLUME, FAULT PLANE AREA, SEISMIC ENERGY, STRAIN, DEFORMATION AND RELATED QUANTITIES

MARKUS BÅTH and SEWERYN J. DUDA

Ricevuto il Gennaio 1964

INTRODUCTION.

Benioff initiated strain release studies around 1950. Since that time the same method as originally given by Benioff (1951), has been used by all who have worked in this field, including ourselves. In the original method, strain is proportional to the square root of the released seismic energy. The volume of every aftershock was considered constant and equal to the total volume of the aftershock zone. The fraction of elastic energy converted into seismic energy was also assumed constant. Moreover, an older energy-magnitude formula has been used for consistency reasons, although newer and better formulas have been developed in the meantime. In the present paper an effort is described to improve Benioff's method, especially in the directions mentioned.

NOTATION.

We shall be using the following notation throughout the present paper:

A, A' = constants, cm;

α = dip angle of the fault plane, degrees;

D = deformation, cm^3;

E = seismic wave energy, ergs;

E_1 = seismic wave energy of the largest aftershock in a sequence, ergs;

ϵ = average strain in the focal region of an earthquake;

F = fault plane area, cm^2;

H = vertical extent of aftershock zone, cm;

h = vertical extent of fault plane, cm;

h_1 = width of fault plane, cm;

J = elastic strain energy, ergs;

μ = rigidity, dynes/cm^2;

L = length of aftershock zone, cm;

l = length of fault plane, cm;

log = logarithm to the base 10;

M = earthquake magnitude, equivalent to M_S in Gutenberg & Richter's (1956) notation;

M_1 = magnitude of largest aftershock in a sequence;

q = seismic gain ratio = E/J (same as "loss ratio" of Lomnitz 1963);

S = aftershock area, cm^2;

t = time interval after the main shock, days;

V = earthquake volume, identified with total aftershock volume, cm^3;

V_e = volume of major part of elastic strain energy content, cm^3;

δV = $V - V_e$;

v = volume of tectonic stress field (Lomnitz 1963), cm^3;

p = v/V;

W = width of aftershock area, cm.

EARTHQUAKE VOLUME AND MAGNITUDE.

The earthquake volume is not accessible for direct measurements and it is natural that slightly different definitions have appeared in the literature. Bullen (1953, 1955) identifies the earthquake volume with the strained region, in which the material is near breaking-point prior to an earthquake. Bullen (1963) uses the term focal region to denote the volume from which the major part of the energy is issued. Tsuboi (1956) also defines the earthquake volume as the one where the seismic energy was stored before the earthquake. Gzovsky (1962) calls "the space around the fracture in which a redistribution of elastic

deformation energy is taking place" the earthquake focus. Benioff (1955) defined the original strain zone as the total volume of the aftershocks. Benioff (1962) estimated on the basis of some results by Byerly and DeNoyer (1958) that the strain is confined to a very narrow zone around the fault. However, inferences from geodetic measurements may be of limited applicability because of their necessary limitation to the earth's surface. Unfortunately, there are no measurements available which permit a collocation of the ideas of the two Benioff papers mentioned.

We define earthquake volume as the volume of major energy content and assume this to be identical with Benioff's (1955) original strain zone. Table I summarizes all pertinent information on aftershock sequences we could find in the literature, partly revised, and Fig. 1 shows the corresponding plot of log V versus M. There is no doubt that the earthquake volume increases with magnitude and the straight line in Fig. 1, corresponding to the following least-square solution, represents the data well:

$$\log V = (9.58 \pm 0.51) + (1.47 \pm 0.14)\, M \qquad (1)$$

$$\text{for } 5.3 \leq M \leq 8.7$$

It is interesting to note that V increases with M at about the same rate as the seismic energy E does (Båth 1958). We will assume eq. (1) to be of general validity, e.g. also for the individual shocks in an aftershock sequence.

The scatter in Fig. 1, reflected in the mean errors in eq. (1), has several reasons, which we summarize as follows:

1. Casual errors of M are likely to be less than 1/4 of a magnitude unit, and only of small consequence for our relation.

2. Errors of V may be of greater consequence, because of uncertainties in length, width and depth of aftershock zones. However, as we are naturally only concerned with orders of magnitude of the volume, these uncertainties are also only of minor importance. In the sequences used, there are some variations in the magnitude range and time interval

considered, but these have practically no influence on the result. Recent observations of free oscillations of the earth and of surface waves have permitted an estimate of the fault length (Benioff, Press and Smith 1961; Press, Ben-Menahem and Toksöz 1961, Ben-Menahem and Toksöz 1962), indicating that the length of the aftershock area exceeds the original fault length only by some 10 percent, agreeing with independent data for Kern County 1952, a systematic error of no consequence here. Information from geological expeditions is also in good accord with our assumption. The percentage error of the vertical dimension is somewhat greater than for the other two.

3. Systematic variations of V may exist in comparing different earthquake regions. Unfortunately, very little information is available on this point, except for a few hints. Duda (1963) found indication for a more brittle rheological behaviour in Chile than in the Aleutian Islands or Kamchatka. The comparatively low volume found for the Kern County earthquake may be explained by a reduced shear strength because of many fractures and minor faults in the area (Benioff 1955) or more specifically by the intervention of the Edison fault into the activity on the White Wolf fault (Duda and Båth 1963).

It must be understood that relation (1) is a simplification of real conditions, at least to the same extent that any relation between E and M is a simplification. As indicated in point 3. above, there are certainly a number of other factors entering any such relation as well, but at present these are impossible to take into account.

Moreover, it must be emphasized that even in case the aftershock total volume V would be essentially larger than the volume V_e where the major part of the elastic strain energy is stored, i.e.

$$V = V_e + \delta V \qquad (2)$$

our relation is correct up to a constant factor, provided $\delta V/V_e$ is independent of magnitude.

FAULT PLANE AREA, AFTERSHOCK AREA AND MAGNITUDE.

Before proceeding we shall also consider some other relations between geometrical properties of an earthquake and its magnitude.

Berckhemer (1962) gave a relation between fault plane area and magnitude:

$$\log F = 0.45 + 1.7\ M \qquad (3)$$

$$\text{for } 5.5 \leq M \leq 8.0$$

Although his data would suggest introduction of an M^2-term in this relation, especially for $M < 6$, where unfortunately the data are very scanty, only the linear relation (3) is given in Berckhemer's paper.

The aftershock area S has been related to the magnitude of the main shock, especially by several Japanese seismologists. The latest published relation, known to us, was given by Utsu and Seki (1955), based on 39 aftershock sequences in and near Japan:

$$\log S = 5.99 + 1.02\ M \qquad (4)$$

According to Utsu (1961) this relation is confirmed by aftershock sequences from other areas as well, except for the Kamchatka 1952 sequence, which had an exceptionally large area. Fig. 1 shows the straight line (4) together with some of our observations. The agreement is not very satisfactory, and a new relation was derived from our observations by the least-square method:

$$\log S = (4.95 \pm 0.43) + (1.21 \pm 0.18)\ M \qquad (5)$$

This relation is certainly based on only six observations, which, however, represent a number of quite different earthquake regions and line up remarkably well on a straight line, again with exception for Kern County 1952, which is low.

From the geometry of Fig. 2, showing the fault plane of the main shock inside the total aftershock volume, in the shape of a parallelopiped, we have immediately the following relations:

$$V = L\ W\ H\ ; \quad S = L\ W\ ; \quad F = \ell h_1\ ; \quad h_1 = h/\sin\alpha \qquad (6)$$

For the cases with available information on α (Table I), it is obvious

that $\sin \alpha \geq 0.87$, and therefore we can put h_1 approximately equal to h. For obvious reasons, $F/LH \leq 1$. This ratio is plotted against magnitude in Fig. 1 (see also Table I). There is evidently some indication of an increase of F/LH with M, approaching unity for the largest shocks, as shown by the dotted curve in Fig. 1.

ELASTIC STRAIN ENERGY AND SEISMIC ENERGY.

Combining eq. (1) with Båth's (1958) energy- magnitude formula:

$$\log E = (12.24 \pm 1.35) + (1.44 \pm 0.20)\, M \qquad (7)$$

we find that

$$\log (E/V) = (2.66 \pm 1.86) - (0.03 \pm 0.34)\, M \qquad (8)$$

This means that the seismic energy density, i.e. the seismic energy per unit volume, is independent of the magnitude. Fig. 1 shows the straight line (8) together with our observations. Similar results have been expressed by Pshennikov (1962).

From the values in Table I we find that for circum-Pacific earthquakes, cases 1-6, the average value of $\log (E/E_1) = 1.73 \pm 0.29$, corresponding to an average of $M - M_1 = 1.2 \pm 0.2$, an excellent confirmation of the so-called Båth's law (Richter 1958, p. 69). This agrees with No. 10 (Outer Mongolia).

The source from which earthquakes derive their energy, i.e. the potential energy within the earth, is not accessible to direct measurements. The potential energy consists mainly of the elastic strain energy, even if some other kinds of potential energy, due to the state of the material, cannot be excluded, especially at greater depth (Benioff 1963). So far we have had no information on the seismic gain ratio $q = E/J$ and its possible relation to magnitude. Benioff (1951) assumed q to be constant and put it equal to unity.

Lomnitz (1963) expressed the hypothesis that q is related to F and v in the following way:

$$q = A' \frac{F}{v} = A \frac{F}{V} \qquad (9)$$

with A' and A = A'/p assumed by us to be independent of the magnitude. Even if the expression (9) seems to be reasonable, we have to remember that it is nothing more than a hypothesis. Then, q would increase with magnitude at the same rate as F/V (Table II). Assuming that q has reached its maximum value, i.e. unity, for the largest shocks (here taken as M = 8.7), as inferred from our result concerning magnitude variation of F/LH, we get the maximum value of A = 1.35×10^7 cm. With this value of A together with eqs (9), (3) and (1) we find that

$$\log q = (-2.00 \pm 0.51) + (0.23 \pm 0.14)\, M \qquad (10)$$

We see from Table II that about seven times more of the elastic strain energy is converted into seismic energy for an earthquake of magnitude 8.7 as for one of magnitude 5.0.

From the definition of q and eq. (9) we get

$$\log J = \log E - \log A - \log F + \log V \qquad (11)$$

Inserting eqs (1), (3), (7) and A = 1.35×10^7 cm, we find that

$$\log J = (14.24 \pm 1.86) + (1.21 \pm 0.34)\, M \qquad (12)$$

Under the same conditions we immediately derive the following expression for the elastic strain energy density:

$$\log (J/V) = (4.66 \pm 1.35) - (0.26 \pm 0.20)\, M \qquad (13)$$

There is no significant variation of J/V with M, just as the case is with E/V, eq. (8).

STRAIN RELEASE AND DEFORMATION CHARACTERISTICS.

With reference to Båth and Benioff (1958) we have the following formula for calculation of the average strain ε:

$$E = \tfrac{1}{2} q \mu \varepsilon^2 V \qquad (14)$$

The strain is in this formula composed of a distortional and a dilatational part, which cannot be separated from each other. Als the volumes of distortional and dilatational strain energy storage have to be assumed equal.

In the light of the results described earlier in this paper, we suggest the following improvements of Benioff's (1951) original method in the application of eq. (14):

1) V will vary with M according to (1), instead of being assumed constant;

2) q is assumed to vary with M according to (9), as an alternative to the still plausible assumption of constant q = 1 according to Benioff (1951);

3) E varies with M according to (7), being the most reliable energy-magnitude formula so far produced, in excellent agreement with an independent result by Gutenberg and Richter (1956).

The rigidity μ will still be assumed constant = 6×10^{11} dynes/cm^2, valid for the upper part of the earth where the earthquakes considered took place. However, there are some indications that μ depends on the stress state of the material (Duda 1962).

Solving eq. (14) for ε and considering only the positive root, which may be approximately correct as long as we consider only one earthquake area at a time, we have

$$\varepsilon = \left(\frac{2E}{q\mu V}\right)^{\frac{1}{2}} \tag{15}$$

We consider two cases, depending upon the expression for q chosen.

1) $q = A\frac{F}{V}$, i.e. eq. (9). Eq. (15) then becomes

$$\varepsilon = \left(\frac{2E}{A\mu F}\right)^{\frac{1}{2}} \tag{16}$$

Applying eqs (7) and (3) and putting $A = 1.35 \times 10^7$ cm, we obtain that

$$\log \varepsilon = -(3.41 \pm 0.68) - (0.13 \pm 0.10)\, M \tag{17}$$

2) q = 1. In this case, (15) becomes

$$\varepsilon = \left(\frac{2E}{\mu V}\right)^{\frac{1}{2}} \tag{18}$$

Inserting eqs (1) and (7), we find that

$$\log \varepsilon = -(4.41 \pm 0.93) - (0.015 \pm 0.17)\, M \tag{19}$$

The resulting eqs (17) and (19) agree in the sense that the strain has no significant variation with magnitude. See Table II.

This result may seem surprising at first sight. However, it is in better accord with general inferences from rock behaviour under stress than that strain should increase rapidly with magnitude. The essential difference between large and small shocks is not to be found in the strain release but in the volume within which a release takes place at the same time. The rock can store a certain amount of strain before it breaks. If strain were magnitude-dependent this would mean that each rock should be able to store strain corresponding to a certain minimum earthquake magnitude. It is then a justified question why in seismic areas not only shocks above a certain magnitude exist, but also a far greater number of smaller shocks. Our result of constant strain but magnitude-dependent volume seems to meet these problems.

In order to study creep phenomena in aftershock sequences, Benioff (1951) initiated the construction of strain release characteristics. Under the term strain, we understand deformation per unit volume, by virtue of the fact that deformation in the neighbourhood of any point can always be expressed as the resultant of simple extensions (called principal extensions) in three mutually perpendicular directions (called the principal axes of strain). See Bullen (1963, p. 17). We still consider a strain characteristic as valuable in describing the behaviour of the rock under stress, but we are now unable to construct any such curve because of the following facts:

1) As strain is independent of magnitude, we should need to know all aftershocks, especially the large number of small ones, to be able to construct a reliable curve. However, such information is naturally not available.

2) Considering strain, we are only concerned with one particular unit volume. It would be incorrect to add strains from quite different volumes, as would be the case if strains of many small aftershocks in different parts of a large aftershock region were added.

For these reasons, we have to refrain from tracing any strain release characteristics. On the other hand, deformation characteristics,

referring to the whole aftershock volume can be traced because of the theorem mentioned (Bullen 1963, p. 17) and because neither of the objections above is applicable in this case. In addition, as focal mechanisms are very similar or closely related within one and the same earthquake area (Båth 1952), the principal axes of strain are approximately conserved within such an area and it will be justified to add deformations from different parts of the same area. The deformation characteristic gives a true picture of the real happenings in the aftershock zone and has an obvious interest from the tectonophysical point of view. Of course, under Benioff's (1951) assumptions the strain and deformation characteristics had the same shape, differing only by a constant factor.

Using eq. (18), i.e. assuming $q = 1$, we have

$$D = \varepsilon V = \left(\frac{2EV}{\mu}\right)^{\frac{1}{2}} \tag{20}$$

which in combination with eqs (1) and (7) becomes

$$\log D = (5.17 \pm 0.93) + (1.46 \pm 0.17)\, M \tag{21}$$

E, V and D all increase with M at about the same rate.

Using eq. (21) on two aftershock sequences for which the material has been published earlier, i.e. Aleutian Islands 1957 (Duda 1962) and Chile 1960 (Duda 1963), we have constructed the deformation characteristics shown in Fig. 3.

The accumulated deformation in the aftershock zones can be represented analytically as follows:

Aleutian Islands 1957:

$$\left.\begin{array}{lll} \text{1st branch} & 0.031 \leq t \leq 1.36 & D = (1.48 + 0.96 \log t) \times 10^{16} \\ \text{2nd branch} & 1.36 \leq t \leq 6.4 & D = (1.05 + 4.19 \log t) \times 10^{16} \\ \text{3rd branch} & 6.4 \leq t \leq 39 & D = (1.95 + 3.07 \log t) \times 10^{16} \\ \text{4th branch} & 39 \leq t \leq 1266 & D = (3.67 + 1.99 \log t) \times 10^{16} \end{array}\right\} \tag{22}$$

Chile 1960:

$$\begin{array}{lll} \text{1st branch} & 0.122 \leq t \leq 7.90 & D = (0.41 + 0.42 \log t) \times 10^{16} \\ \text{2nd branch} & 7.90 \leq t \leq 952 & D = \left[0.79 + 5.03\,(1 - e^{-0.12(t-7.9)^{\frac{1}{2}}})\right] \times 10^{16} \end{array} \tag{23}$$

The 2nd-4th branches of the Aleutian Islands deformation characteristic are only to be understood as straight-line approximations for an exponential curve, extending over the entire interval $1.36 \leq t \leq 1266$, i.e. corresponding to the second branch for the Chile 1960 characteristic. Our improved methods have had the consequence that the earlier published characteristics are somewhat changed, and it is very interesting to note that the behaviour is analogous in the two sequences studied here. This behaviour was also evident for quite a number of aftershock sequences studied by the old method. Thus, the sequences of Long Beach 1933, Imperial Valley 1940 and Hawke's Bay 1931 exhibited this behaviour (Benioff 1951), also some others reported in the same paper but interpreted differently by Benioff, i.e. Manix 1947, Nevada 1932 and less clear Signal Hill 1933. Other examples are Kern County 1952 (Benioff 1955) and San Francisco 1957 sequences (Tocher 1959). It remains to be seen if the improved technique presented in this paper will bear out that this is a general behaviour for aftershock sequences.

CONCLUSIONS.

We can summarize the results of the present investigation in the following points.

1. Earthquake volume, identified with the total aftershock volume, increases with magnitude according to the following equation:

$$\log V = (9.58 \pm 0.51) + (1.47 \pm 0.14)\, M$$

2. The ratio of fault plane area to the vertical section through the aftershock zone, i.e. F/LH, increases with magnitude, approaching unity for the largest shocks.

3. The aftershock area increases with magnitude according to the following equation:

$$\log S = (4.95 \pm 0.43) + (1.21 \pm 0.18)\, M$$

4. The seismic gain ratio is expressed as follows, adopting a suggestion

by Lomnitz (1963):

$$q = \frac{E}{J} = A \frac{F}{V}$$

Under this assumption, q increases with magnitude.

5. The seismic energy density, E/V, as well as the elastic strain energy density, J/V, are independent of magnitude.

6. Strain is independent of magnitude. Therefore, the main difference between large and small earthquakes is not to be found in the strain but in the total volumes involved, This is in agreement with Tsuboi's (1956) results.

7. The deformation, i.e. the total strain in the aftershock zone, increases with magnitude according to the following formula:

$$\log D = (5.17 \pm 0.93) + (1.46 \pm 0.17)\, M$$

i.e. at almost exactly the same rate as the seismic energy E or the volume V.

8. By means of the improved method given in this paper, some earlier strain release characteristics (Aleutian Islands 1957 and Chile 1960 sequences) are reconstructed, now as deformation characteristics. It appears likely that most aftershock sequences exhibit similar deformation-time characteristics.

ACKNOWLEDGMENT.

The research reported in this paper was carried out at the Seismological Institute, Uppsala, with the support and sponsorship of the Cambridge Research Laboratories of the Office of Aerospace Research, United States Air Force, through its European Office, as part of the Advanced Research Project Agency's project Vela Uniform, under contract AF 61(052)-588.

Seismological Institute, Uppsala, Sweden

January, 1964

SUMMARY

An effort is made to improve Benioff's method for investigation of strain release in aftershock sequences. The improvements may be summarized as follows:

1. Earthquake volume increases with magnitude, instead of being constant. A relation is given, relating volume to magnitude.
2. A revised energy-magnitude formula is used.
3. The seismic gain ratio, i.e. the ratio between seismic energy and elastic strain energy, probably increases with magnitude, instead of being constant. Likewise, the ratio of fault plane area of the main shock to the vertical section through the aftershock volume increases with magnitude.
4. The seismic energy density, the elastic strain energy density as well as strain are independent of magnitude.
5. The deformation, i.e. the total strain in the aftershock zone, increases with magnitude at the same rate as seismic energy and volume do.

As a consequence of these improvements some earlier published strain release characteristics are reconstructed, this time as deformation characteristics instead.

REFERENCES

Båth M., Initial Motion of the First Longitudinal Earthquake Wave Recorded at Pasadena and Huancayo. "Bull. Seism. Soc. Amer.", 42, 175-195, (1952).

Båth M., The Energies of Seismic Body Waves and Surface Waves. "Contributions in Geophysics in Honour of Beno Gutenberg", 1, 1-16, Pergamon Press, London, (1958).

Båth M. and Benioff H., The Aftershock Sequence of the Kamchatka Earthquake of November 4, 1952. "Bull. Seism. Soc. Amer.", 48, 1-15, (1958).

Benioff H., Earthquakes and Rock Creep, Part I: Creep Characteristics of Rocks and the Origin of Aftershocks. "Bull. Seism. Soc. Amer.", 41, 31-62, (1951).

—— Mechanism and Strain Characteristics of the White Wolf Fault as indicated by the Aftershock Sequence. "Calif. Dept. Nat. Resources, Division of Mines, Bull.", 171, Pt II, 199-202, (1955).

—— Movements on Major Transcurrent Faults. "Continental Drift", International Geoph. Ser., 3, 103-134, Academic Press, New York and London, (1962).

—— Source Wave Forms of Three Earthquakes. "Bull. Seism. Soc. Amer.", 53, 893-903, (1963).

Benioff H., Press F. and Smith S., Excitation of the Free Oscillations of the Earth by Earthquakes. "Jour. Geoph. Res.", 66, 605-619, (1961).

Ben-Menahem A. and Toksöz M. N., Source-Mechanism from Spectra of Long-Period Seismic Surface-Waves, 1. The Mongolian Earthquake of December 4, 1957. "Jour. Geoph. Res.", 67, 1943-1955, (1962).

Berckhemer H., Die Ausdehnung der Bruchfläche im Erdbebenherd und ihr Einfluss auf das seismische Wellenspektrum. "Gerl. Beitr. z. Geoph.", 71, 5-26, (1962).

Bullen K. E., On Strain Energy and Strength in the Earth's Upper Mantle. "Trans. Amer. Geoph. Union", 34, 107-109, (1953).

—— On the Size of the Strained Region prior to an Extreme Earthquake. "Bull. Seism. Soc. Amer.", 45, 43-46, (1955).

—— " An Introduction to the Theory of Seismology." 381 pp., Cambridge Univ. Press, (1963).

Byerly P. and DeNoyer J., Energy in Earthquakes as Computed from Geodetic Observations. "Contributions in Geophysics in Honour of Beno Gutenberg", 1, 17-35, Pergamon Press, London, (1958).

Duda S. J., Phänomenologische Untersuchung einer Nachbebenserie aus dem Gebiet der Aleuten-Inseln. "Freiberger Forschungshefte",

C 132, 1-90, (1962).

—— Strain Release in the Circum-Pacific Belt: Chile 1960. "Jour. Geoph. Res.", 68, 5531-5544, (1963).

Duda S. J. and Båth M., Strain Release in the Circum-Pacific Belt: Kern County 1952, Desert Hot Springs 1948, San Francisco 1957. "Geophys. Jour. Roy. Astr. Soc.", 7, 554-570, (1963).

Gutenberg B. and Richter Ch., Magnitude and Energy of Earthquakes. "Annali di Geofisica", 9, 1-15, (1956).

Gzovsky M. V., Tectonophysics and Earthquake Forecasting. "Bull. Seism. Soc. Amer.", 52, 485-505, (1962).

Lomnitz C., Estimation Problems in Earthquake Series. Paper presented at the Upper Mantle Symposium, XIII General Assembly of IUGG, Berkeley, 15 pp., (1963).

Press F., Ben-Menahem A. and Toksöz M. N., Experimental Determination of Earthquake Fault Length and Rupture Velocity. "Jour. Geoph. Res.", 66, 3471-3485, (1961).

Pavlenkov K. W., Some Peculiarities of the Aftershocks in the Baikal Region and Mongolia (in Russian). "Geology and Geophysics", 4, 119-121, (1962).

Richter C. F., "Elementary Seismology". 768 pp., W. H. Freeman and Co., San Francisco, (1958).

Richter C. F., Allen C. R. and Nordquist J. M., The Desert Hot Springs Earthquakes and their Tectonic Environment. "Bull. Seism. Soc. Amer.", 48, 315-337, (1958).

Tocher D., Seismographic Results from the San Francisco Earthquakes of 1957. " Calif. Dept. Nat. Resources, Division of Mines, Special Report", 57, 59-71, (1959).

Tsuboi Ch., Earthquake Energy, Earthquake Volume, Aftershock Area, and Strength of the Earth's Crust. "Jour. of Phys. of the Earth", 4, 63-66, (1956).

Utsu T., A Statistical Study on the Occurrence of Aftershocks. "Geoph. Mag.", 30, 521-605, (1961).

Utsu T. and Seki A., Relation between the Area of the Aftershock Region and the Energy of the Main Shock. "Jour. Seism. Soc. Japan, Ser. II", 7, 233-240, (1955).

Table I - DATA FOR EARTHQUAKES USED IN THIS STUDY

No.	1	2	3	4	5	6	7	8	9	10	11
Date	22 Mar, 1957	4 Dec, 1948	21 July 1952	9 Mar, 1957	4 Nov, 1952	22 May, 1960	10 Apr, 1958	6 Feb, 1957	29 Aug, 1959	4 Dec, 1957	27 June, 1957
Origin time, GMT	19 44 21.0	15 43 16.7	11 52 14.3	14 22 27.5	16 58 26	18 55 57 19 10 37 19 11 17	10 55 31	20 34 55	17 03 10	03 37 45	00 09 28
Lat. Long.	37.7 N 122.5 W	33.9 N 116.4 W	35.0 N 119.0 W	51.3 N 175.8 W	52.8 N 159.5 E	38-39.5 S 73.5-74.5W	51.5 N 99 E	50 N 105.5 E	52 N 106.5 E	45.5 N 99.5 E	56,5 N 116 E
Region	San Francisco	Desert Hot Springs	Kern County	Aleutian Islands	Kamchatka	Chile	Outer Mongolia	Lake Baikal	Lake Baikal	Outer Mongolia	N Lake Baikal
M	5.3	6.5	7.7	8 1/4	8.5	8.7	5.7	6.4	6.7	7.8	7.9
E, eq.(7) 10^{20} ergs	0.741	39.8	2140	13200	30200	58900	2.82	28.8	77.6	2950	4170
V, 10^{20} cm^3	0.00175	0.0460	0.730	154	148	303	(0.04)	(0.04)	0.79	18	11
E/V erg/cm^3	423	865	2930	86	204	194	71	720	98	164	379
S, 10^{12} cm^2	0.25	13	21	1540	2470	4030					
M_1	4.4	4.9	6.4	7.3	7 1/4	7.5				6.5	
$\log(E/E_1)$	1.30	2.30	1.87	1.37	1.80	1.73				1.87	
α, degrees	77.6-89.7	$\geq$66	60-66	86	79-89						
L x H 10^{12}cm^2	0.63	6.3	21	1330	620	1130					
F, eq.(3) 10^{12}cm^2	0.00288	0.316	34.7	299	794	1740					
F/LH	0.005	0.050	1.65	0.22	1.28	1.54					
Reference	Tocher (1959)	Richter, Allen, Nordquist(1958)	Benioff (1955)	Duda (1962)	Båth, Benioff (1958)	Duda (1963)	Pshenni-kov(1962)	Pshenni-kov(1962)	Pshenni-kov(1962)	Pshenni-kov(1962)	Pshenni-kov(1962)

Table II - VARIATION OF GAIN RATIO, ENERGY, STRAIN AND DEFORMATION WITH MAGNITUDE

M	F/V	q	E	J	J/V	ε	ε	D
	eqs (1) and (3)	eq. (10)	eq. (7)	eq. (12)	eq. (13)	eq. (17)	eq. (19)	eq. (21)
	$10^{-8}cm^{-1}$		$10^{20}ergs$	$10^{20}ergs$	$10^{3}ergs/cm^{3}$	10^{-5}	10^{-5}	$10^{13}cm^{3}$
5.0	1.05	0.142	0.28	1.95	2.29	8.73	3.28	0.3
5.5	1.36	0.184	1.45	7.85	1.70	7.51	3.22	1.6
6.0	1.78	0.240	7.58	31.6	1.26	6.47	3.17	8.5
6.5	2.32	0.313	39.8	127	0.93	5.57	3.11	46
7.0	3.02	0.408	209	513	0.69	4.80	3.06	245
7.5	3.94	0.532	1090	2060	0.51	4.13	3.01	1320
8.0	5.13	0.693	5750	8320	0.38	3.56	2.96	7110
8.5	6.68	0.902	30200	33500	0.28	3.06	2.90	38200
8.7	7.43	1.000	58900	58500	0.25	2.88	2.88	74800

(Captions for the figures)

Fig. 1 - Various earthquake parameters plotted against magnitude. The circles are our observations, using reference numbers of Table I.

Fig. 2 - Schematical picture of fault plane inside aftershock volume.

Fig. 3 - Deformation characteristics for the Aleutian Islands 1957 and Chile 1960 aftershock sequences.

Fig. 1

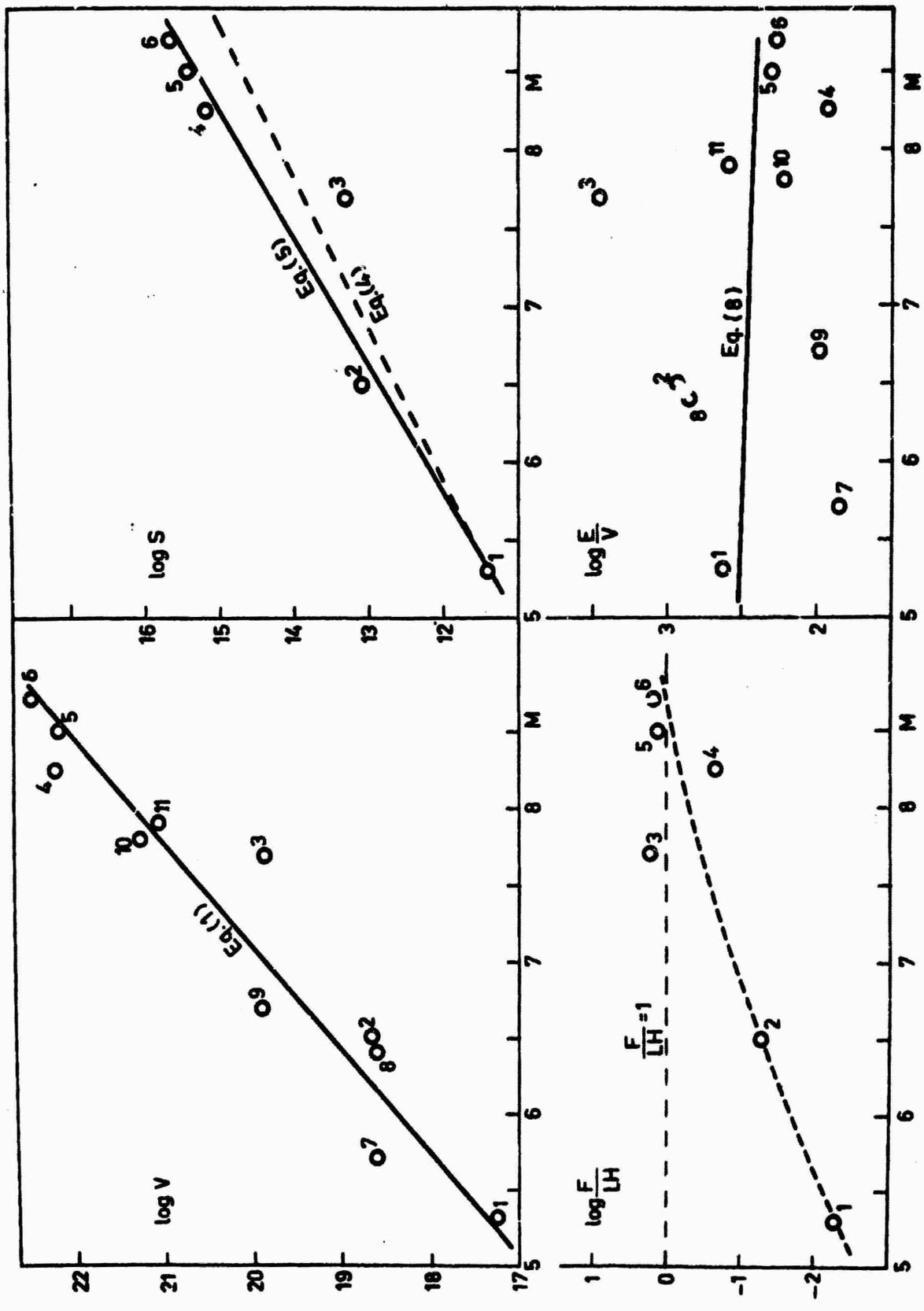

Fig. 2

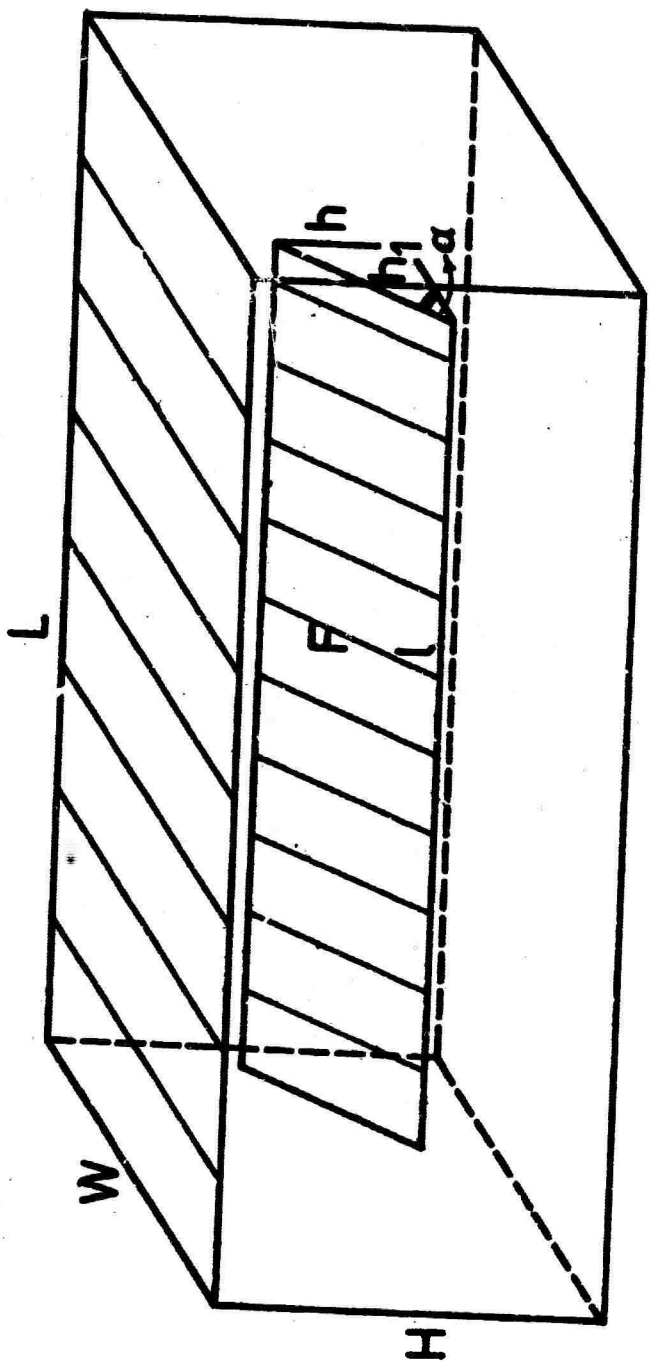

Fig. 3

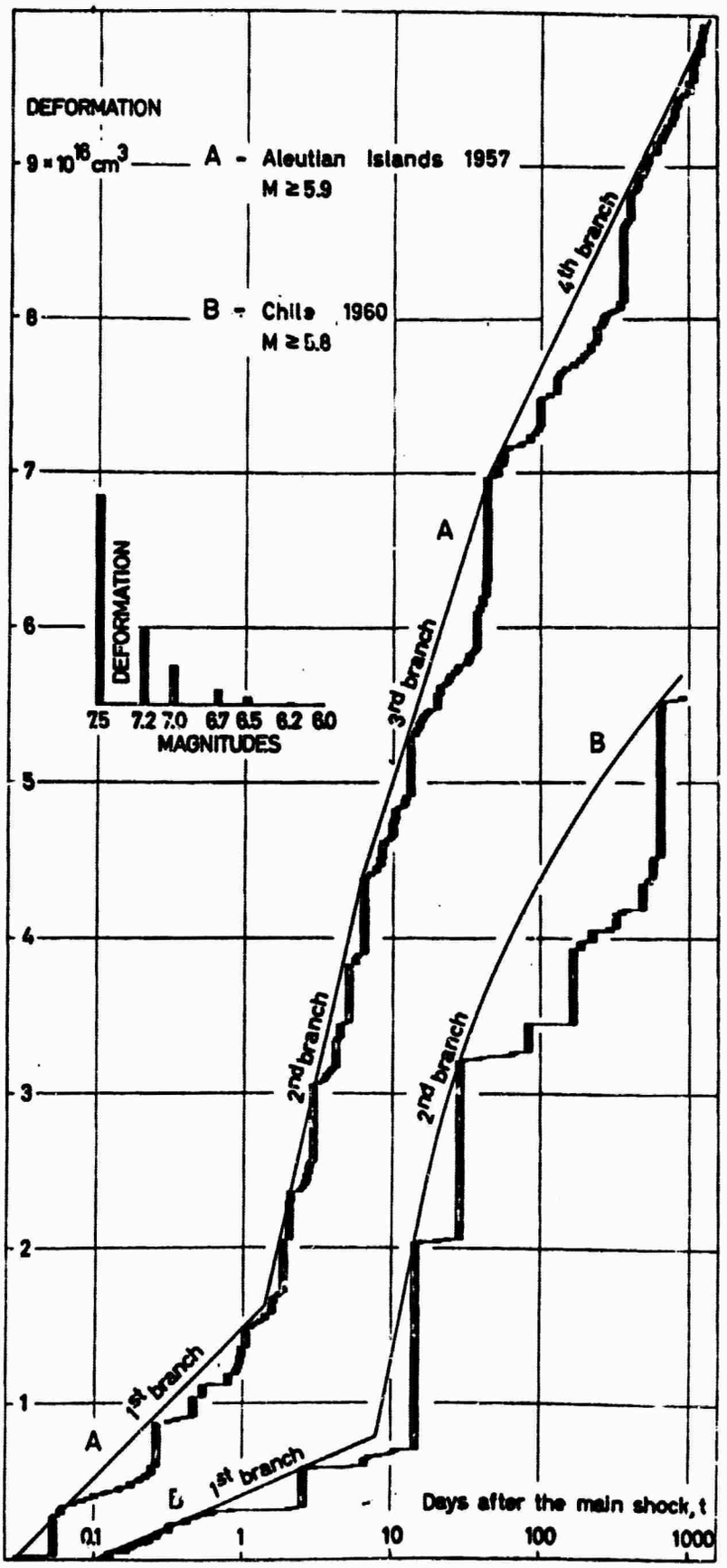
DEFORMATION
9 × 10^16 cm^3
A - Aleutian Islands 1957
M ≥ 5.9
B - Chile 1960
M ≥ 5.8
DEFORMATION
7.5 7.2 7.0 6.7 6.5 6.2 6.0
MAGNITUDES
1st branch
2nd branch
3rd branch
4th branch
A
B
Days after the main shock, t
0.1
1
10
100
1000

A P P E N D I X II

THE STRESS FIELD AROUND A FAULT ACCORDING TO A PHOTOELASTIC MODEL EXPERIMENT

Seweryn J. Duda

Seismological Institute

University of Uppsala

Uppsala, Sweden

Contract No. AF 61(052)-588

January 15, 1964

pared for

GEOPHYSICS RESEARCH DIRECTORATE

AIR FORCE CAMBRIDGE RESEARCH LABORATORIES

OFFICE OF AEROSPACE RESEARCH

UNITED STATES AIR FORCE

BEDFORD, MASSACHUSETTS

WORK SPONSORED BY ADVANCED RESEARCH PROJECTS AGENCY

PROJECT VELA-UNIFORM

ARPA Order No. 180-62, Amendment No. 7

dated 3 Aug. 1961

Project Code No. 8100, Task 86520

Intended for publication in the Geophysical Journal,

Royal Astronomical Society, London

THE STRESS FIELD AROUND A FAULT ACCORDING TO A PHOTOELASTIC MODEL EXPERIMENT

Seweryn J. Duda

(Received 1964 January)

Summary

A report is given of preliminary photoelastic measurements of the two-dimensional stress field around a fault or crack in a plate. The measurements include the following cases: open slit with the uniaxial applied pressure field making an angle of 45° with the slit; closed slit (zone of weakness) with two different thicknesses of the weak zone and again 45° to the external pressure field; the measurements for the weakest slit were made also with an angle of 22.5° to the pressure field. The measured and calculated normal and shear stresses are represented in graphical form. The results provide explanations for some earthquake characteristics, for example distribution of shear stress and patterns of geographical extension of seismic activity during an aftershock sequence.

1. Introduction

A knowledge of the stress field around tectonic faults is of great tectonophysical importance. However, generally only indirect methods are at our disposal for its determination. These methods work with simplified models, either mathematical models or laboratory models. We shall only be considering two-dimensional models.

Inglis (1913) gave the analytical solution for the two-dimensional stress state around an elliptical hole in an infinite plate for different external stresses. Anderson (1951) applied these results to a degenerated ellipse, i.e. with one axis equal to zero, under the following boundary conditions:

1. external pressure and tension, mutually perpendicular, act under 45° to

the fracture, so that a pure shear stress arises parallel to the fracture;
2. there is no transmission of shear stress across the fracture.
The principal stresses along the fracture were found to be zero in the middle, increasing to infinity towards its ends. This is a first approximation of a tectonical fault in a pure shear stress field and furnishes a good explanation of some observed earthquake patterns (Duda 1962), especially the accumulation of epicenters and even more of seismic energy towards the ends of a fault. However, Anderson's model is time-independent, whereas an aftershock sequence continues for a considerable time. Therefore, only the time-integral of the aftershock pattern can be compared with Anderson's model.

The condition 2. above is a severe simplification of natural conditions. A real fault has to be understood as a zone of weakness, still able to transmit shear stresses from one side to the other. A generalization of Anderson's model introducing friction at the fault would lead to considerable mathematical difficulties, and to our knowledge this problem has not been analytically solved.

In the present research we have tried to solve this problem by an analogue processing, using the photoelastic method for determination of the stress field around a rectilinear, finite fracture in a transparent plate. Our boundary conditions are:
1. external homogeneous pressure field acting parallel to the plate under angles of 45° and 22.5° resp. to the fracture;
2. transmission of shear stress across the fracture.

The application of a uniaxial, homogeneous pressure field on the plate represents a more general analogy to tectonical conditions than a pure shear stress field parallel to the fault. At any point in the orogenetic shell, the two principal stresses will in most cases be two pressures, generally unequal. Such a pressure field may be divided into a hydrostatic pressure and a residual pressure, of which only the latter is of importance for tectonic movements. Its action will depend on the angle it forms with the fault. If

the pressure is perpendicular to the fault, this will be closed and no earthquake occurs. If they are parallel, the fault will be opened or bent, and no seismic activity will be observed either. Seismic activity will be expected for all other angles, being a maximum for an angle of 45°.

The photoelastic method has so far been used only exceptionally in seismology or general geophysics, as e.g. for studies of seismic wave propagation (Thomson 1963) or of stress distribution in models of wells and galleries (Schmidt 1961).

2. The photoelastic method

Extensive treatments of the photoelastic method have been given by Hiltscher (1958) and by Frocht (1960). The basic physical principle of the method is that some transparent materials, when loaded, show double refraction of light. The velocity of light changes in a loaded model from point to point and depends upon its direction of propagation. Thus a light beam leaving the loaded model will be polarized. In a two-dimensional model, like a plate, loaded parallel to its plane, a light beam will be plane-polarized at every point in the directions of the principal stresses. The two light components will have different velocities, proportional to the respective principal stress.

We introduce the following notation:

σ_1, σ_2 = principal stresses;

R_t = relative retardation or phase difference, expressed in wave lengths;

C = stress-optic coefficient (Frocht 1960);

d = plate thickness;

Δd = change of plate thickness due to load;

k = lateral constant (Hiltscher 1963).

Then, the following two equations are valid:

$$R_t/d = C(\sigma_1 - \sigma_2) \qquad (1)$$

and

$$\sigma_1 + \sigma_2 = k\Delta d/d \qquad (2)$$

The relative retardation and the directions of the principal stresses are measured in a polariscope (Figure 1). Eq. (1), called the stress-optic law in two dimensions, provides a possibility to determine the difference of the principal stresses, if R_t is measured and d and C are known.

The sum of the principal stresses, expressed in eq. (2), can be determined by different mechanical, optical or electrical methods. In our experiments we used the very efficient and accurate lateral extensometer after Hiltscher (Figure 2) for the measurement of the thickness change Δd. Knowing k and d, we can calculate the sum of the principal stresses from (2). Figure 3 shows schematically the complete apparatus used for the photoelastic measurements.

The described measurements and eqs (1) and (2) reduce the problem to express stresses in any coordinate system to a matter of calculation.

3. Description of our experiments

Four different models, all being transparent plates made of Araldite D, were measured by the photoelastic procedure (Table 1 and Figure 4). The slits were in every case located in the center of the plate and orientated along a diagonal. Model O (where O stands for "open") had an open slit, the other models close slits, consisting of cuts from either side, 0.4 cm deep in Model A and 0.45 cm deep in Models B and C. Profiles I and II were parallel to the slit and profile V perpendicular to it. Profiles III and IV, located symmetrically to I and II with respect to the slit, do not need to be measured for symmetry reasons.

Under load, the slit in Model O is expected to close and friction between its walls to arise. This corresponds to a fault after a rupture of the material along the fault plane. As it is impossible to know, if the slit is

first closed and then friction arises or if the walls are first displaced and then touch each other, the three other models were made. In these the slit corresponds to a zone of weakness, the strength being 1/5 of the surrounding medium in Model A and 1/10 in Models B and C.

In case of Models A, B and C there is really a transmission of shear stress across the slit. These models correspond to pre-existing but blocked faults and the stress field after loading corresponds to the one preceding an earthquake. Model B gives the stress field around the fault nearer the yielding point as compared to Model A. Model C is also relatively near yielding, but the shear stress is no longer the maximum possible for the applied pressure, because the angle between applied pressure and the slit is now only 22.5° as compared to 45° in all preceding cases.

4. Results

We will be using the following notation:

x, y = rectangular coordinates in the plane of the plate, the x-direction coinciding with the direction of applied pressure (Figure 4);

α = angle between σ_1 and positive y-axis, counted positive counterclockwise ($\alpha < \pm 90^{\circ}$);

σ_o = applied pressure, only absolute values used;

σ_x, σ_y = x and y components of pressure (negative) or tension (positive);

τ_o = reference shear stress, chosen = σ_o;

$\tau_{xy} = \tau_{yx}$ = shear stress, positive for clockwise shear, negative for anti-clockwise shear.

The following formulas are used in the computation:

$$\left.\begin{aligned} \sigma_x &= \frac{\sigma_1 + \sigma_2}{2} - \frac{\sigma_1 - \sigma_2}{2} \cos 2\alpha \\ \sigma_y &= \frac{\sigma_1 + \sigma_2}{2} + \frac{\sigma_1 - \sigma_2}{2} \cos 2\alpha \\ \tau_{xy} &= - \frac{\sigma_1 - \sigma_2}{2} \sin 2\alpha \end{aligned}\right\} \qquad (3)$$

The results are given in graphical form in Figures 5-8. All stress components are expressed in relation to the absolute value of the applied external field, which renders all curves immediately comparable. As the slit has a finite width in Models A, B and C, stress values near the slit are less reliable because of three-dimensional effects. Some of the results need to be specially emphasized and the corresponding remarks are collected in what follows.

a. Profile V, Models O, A, B (Figure 5)

σ_x exhibits a maximum value at some distance from the slit, decreasing both towards and away from the slit. It is a tension, except for Model O, where it is a pressure near the slit. The maximum value of σ_x increases from Model A (far from yielding) to Model B (nearer yielding) and is highest for the Model O (open slit).

σ_y is always a pressure with a maximum value at some distance from the slit, decreasing rapidly towards the slit and approaching σ_o away from the slit.

τ_{xy} has a high positive value far away from the slit, and a high negative value when approaching the slit.

b. Profile I, Models O, A, B (Figure 6)

There is no more any symmetry of σ_x, but the extremities exhibit besides double maxima a high negative value to the left in Figure 6, and a high positive value to the right. This stress distribution corresponds to a tendency of the fault to rotate in the considered external pressure field. This tendency is naturally most pronounced in the case of an open slit.

Also σ_y exhibits asymmetry and decreases near the middle of the open slit far below σ_o. There is no axial symmetry because of the fact that the profile runs at some distance from the slit. A parallel profile on the other side of the slit and at the same distance from it would provide reversed mirror-image curves to those given here. This is true in all cases considered.

The asymmetry of τ_{xy} with bigger absolute values to the right in Figure 6

than to the left for Models A,B is also clear from Figure 4, showing the isochromatics for Model A. Curves of equal colour connect points with equal shear stress, increasing from red to green. A high density of isochromatics corresponds to a rapid increase of the shear stress. In Figure 4, Profile I between points 15 and 21, there is a region of high density of isochromatics, corresponding to the large shear stress in Figure 6. For the open slit, the largest negative shear stress appears on the left side of the profile.

In all models (O,A,B) there are positive as well as negative shear stresses on the left part of Profile I but only negative stresses on the right part. This result may be of importance in the interpretation of fault plane solutions in aftershock sequences.

c. Profile II, Models O, A, B (Figure 7)

The fact that Profile II is at a greater distance from the slit has the result that the stress curves, although similar to those for Profile I, are more smoothed. For instance, the double maxima have disappeared.

d. Profiles V, I, II, Model C (Figure 8)

Model C differs from B only in the angle between applied pressure and the slit. Whereas in Profile V, σ_x shows a shape similar to Models O, A, B, there is a pronounced difference in the shape of the σ_y-curves. For the shear stress along Profile V, the main difference is the negative value of τ_{xy} at the ends of the profile in Model C as compared to Models O, A, B.

The stress curves for Profile II are more smooth as compared with Profile I, just as the case is for the other models. For these two profiles, all stress values are smaller for Model C than for Models O, A, B.

e. General remarks

As we have measurements only along a few profiles, these are naturally insufficient to give a complete two-dimensional picture of the stress distribution around the fault, e.g. in the form of stress isolines. On the other hand, the measured profiles are sufficient to give a clear idea of the main features of the stress distribution.

We have started from a given external pressure field and measured the resulting stress distribution around a fault. Applied to nature, the problem may arise to reverse the procedure, i.e. to start from a number of stress measurements around a fault and to deduce the external pressure field. This is an enormously more difficult problem, and it is not even certain if it has a unique solution.

5. Discussion

The purpose of this report is 1) to present an efficient analoque processing method for investigation of stress distributions around model faults and 2) to present these distributions in a few cases resembling tectonical faults. The ultimate goal is to explain the behaviour of earthquakes. In this preliminary work we like to point out a few results, which already seem to provide explanations for some phenomena found in nature.

1. In the photoelastic model experiments, with improved boundary conditions as compared with earlier mathematical models, the increase of shear stress towards the ends of a fault is confirmed. There is also no longer an infinite shear stress at the fault ends.

2. The shear stress reaches a much higher absolute value at the right end of Profile I, Models A, B (Figure 6) than on the left end. For a profile on the opposite side of the slit, the behaviour is opposite. The strain release density for the Desert Hot Springs aftershocks (Richter, Allen & Nordquist 1958, fig. 6) exhibits a similar pattern in relation to the Mission Creek fault, which may be explained by our finding. This would mean that our two-dimensional stress distribution is a good approximation to the stress field around Mission Creek fault, also that the hypocenters do not vary much in depth. Of course, the aftershocks occur in a material with elastic afterworking, and the strain release density map shows a summary effect in time, whereas the photoelastic material used by us had to be nearly perfectly elastic.

3. In Figure 4, the isochromatics at both ends of the slit have a shape resembling the wings of a butterfly. It is well known from laboratory experiments that the fracture will propagate preferably in the direction of the "butterfly's body" (oral communication by R. Hiltscher). This direction depends strongly on the external pressure field. In an investigation by the present author of the Mongolian aftershock sequence starting on December 4, 1957 (03 37 50 GMT, 45.1°N, 99.4°E) it was found that the aftershocks were distributed along the E-W striking fault of the main shock up to a shock on December 3, 1960 (04 24 18.9 GMT, 42.9°N, 104.4°E). With this shock seismic activity started along a fault extending in SE direction from the eastern end of the old fault, making an angle of 40° with this fault. As explanation for this secondary activity we propose that the primary fault propagated in the direction of the body of the stress "butterfly".

6. Acknowledgments

The research reported in this paper has been carried out at the Seismological Institute, Uppsala, with the support and sponsorship of the Cambridge Research Laboratories of the Office of Aerospace Research, United States Air Force, through its European Office, as part of the Advanced Research Project Agency's Project Vela Uniform, under Contract AF 61(052)-588.

Dr. Markus Båth, Director of the Seismological Institute, Uppsala, proposed to the author the application of the photoelastic method for determination of the stress field around a slit, supported the research in all its stages by discussions and read the manuscript.

Dr. Rudolf Hiltscher, Director of the Photoelastic Laboratory at the Royal Water Power Board, Stockholm, contributed unselfishly by many discussions and instrumental advices.

Some of the models were made in the workshop of the ABEM Prospecting Co., Stockholm. Part of the computation work was made on a digital computer at the Swedish Board for Computing Machinery, Stockholm.

The author wishes to express his most sincere thanks to all persons and institutions mentioned.

Seismological Institute

The University

Uppsala, Sweden

1964 January

References

Anderson, E.M., 1951. The dynamics of faulting, Oliver & Boyd, Edinburgh and London, 206 pp.

Duda, S.J., 1962 Phänomenologische Untersuchung einer Nachbebenserie aus dem Gebiet der Alëuten-Inseln, Freiberger Forschungshefte, C 132, 7-90.

Frocht, M.M., 1960. Photoelasticity, 1, J. Wiley & Sons, New York and London, 411 pp.

Hiltscher, R., 1958. Spannungsmessung mit optischen Mitteln (Spannungsoptik), 19-66, Handbuch der Spannungs- und Dehnungsmessung, Ed. by K. Fink & C. Rohrbach, VDI-Verlag, Düsseldorf, 513 pp.

Hiltscher, R., 1963. Development of the lateral extensometer method in two-dimensional photoelasticity, 43-56, Photoelasticity, Proc. Int. Symp. Ill. Inst. Tech., Chicago, Ill., Oct., 1961, Ed. by M.M. Frocht, Pergamon Press, 294 pp.

Inglis, C.E., 1913. Stresses in a plate due to the presence of cracks and sharp corners, Trans. Inst. Naval Architects, 55, 219-230.

Richter, C.F., Allen, C.R. & Nordquist, J.M., 1958. The Desert Hot Springs earthquakes and their tectonic environment, Bull. Seismol. Soc. Amer., 48, 315-337.

Schmidt, M., 1961. Wertung und Möglichkeiten der Spannungsoptik in der gebirgsmechanischen Forschung, Mitt. Markscheidewesen, Herne, 68, 225-238.

Thomson, K.C., 1963. Full-field seismic modelling, AFCRL-63-685. Terr. Sci. Lab., Proj. 8652, 14 pp.

Table 1

Review of models and measured profiles

Model	Plate dimensions side x side x thickness cm	Slit dimensions length x width x depth cm	Profile I n	Profile I a cm	Profile II n	Profile II a cm	Profile V n	Angle between slit and applied pressure
O	15 x 15 x 1	3 x 0.001 x 1	39	0.3	39	0.9	32	45^{o}
A	18 x 18 x 1	3.8 x 0.1 x 0.8	23	0.5	23	1.5	24	45
B	18 x 18 x 1	3.8 x 0.1 x 0.9	23	0.5	23	1.5	24	45
C	14 x 20 x 1	3.8 x 0.1 x 0.9	23	0.5	23	1.5	24	22.5

n = number of measured points

a = distance from slit

(Captions for the figures)

FIG. 1. - Polariscope after Hiltscher (1958). a = analyzer, p = polarizer with light source.

FIG. 2. - Hiltscher lateral extensometer (Hiltscher 1963) for measurement of plate thickness. pp = plate, mt = measuring tips, ms = micrometer screw, d = dial gauge, s = suspending device of the extensometer and its counterweight c.

FIG. 3. - Loading and measuring device for photoelastic experiments, after Hiltscher (1958). Loading device to the left, front view. Measuring device (polariscope) to the right, side view.

FIG. 4. - Isochromatics for Model A with closed slit, showing the profiles V, I, II and the measuring points in relation to the slit s.

FIG. 5. - Stress components along Profile V, Models O, A, B. The measuring points are indicated on the horizontal scales, in every case starting with point no. 1 at the left end (compare Figure 4). s = slit.

FIG. 6. - Stress components along Profile I, Models O, A, B. s = slit.

FIG. 7. - Stress components along Profile II, Models O, A, B.

FIG. 8. - Stress components in Model C.

Fig.1

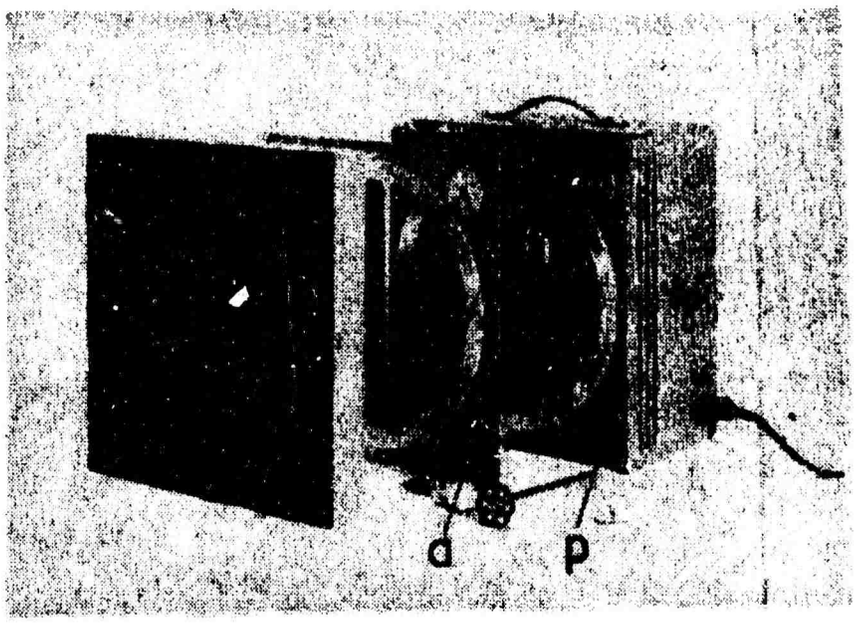

Fig. 2

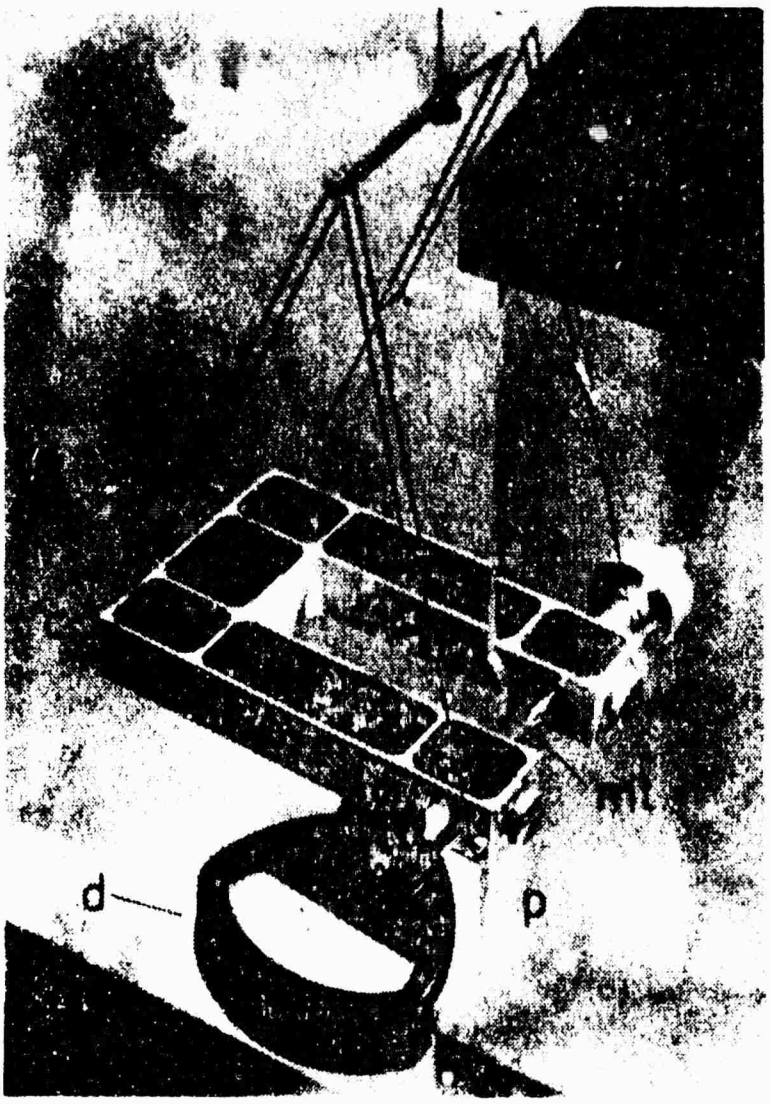

Fig. 3

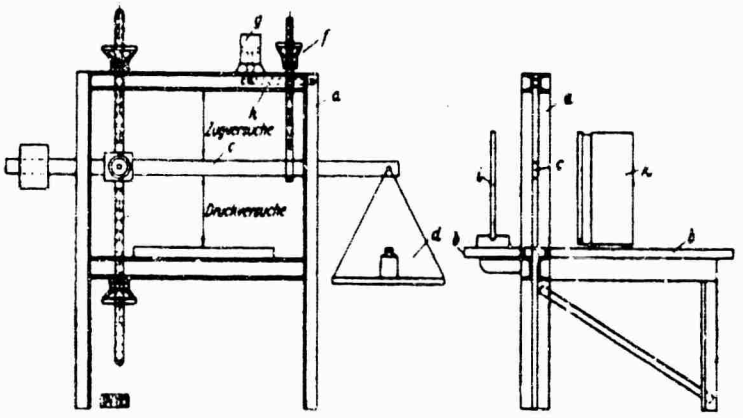

Fig. 4

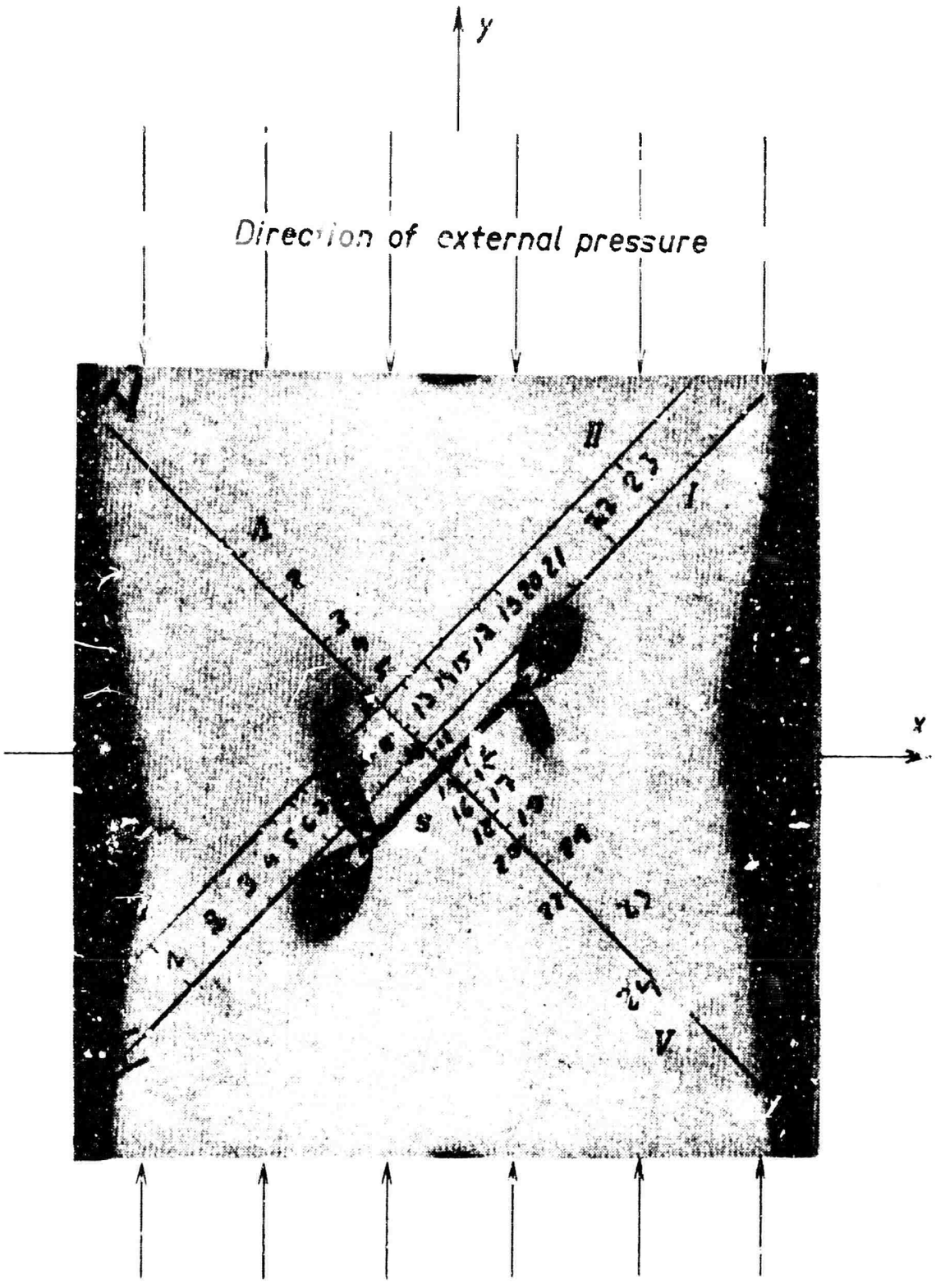

Fig. 5

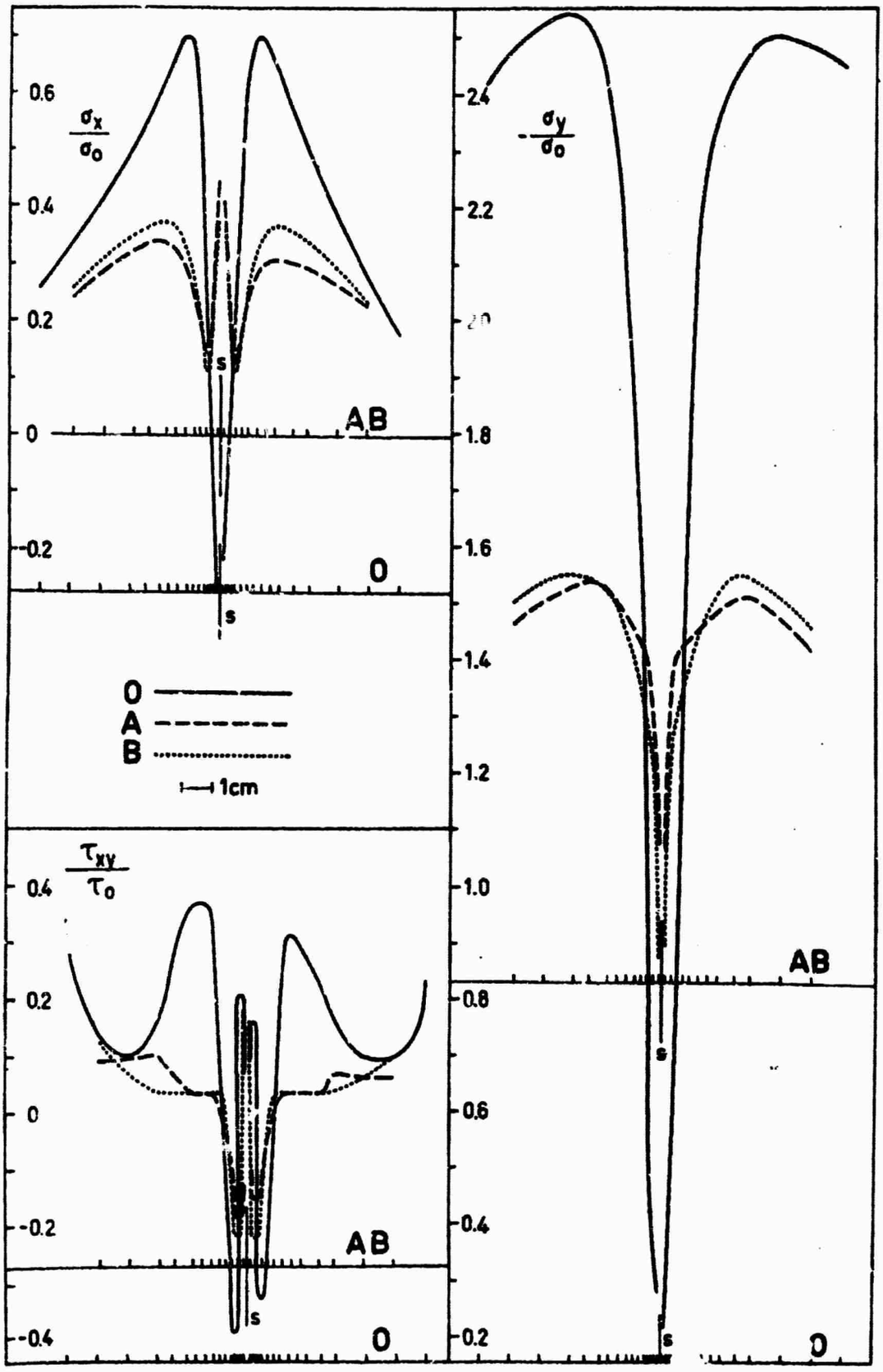
$\frac{\sigma_x}{\sigma_o}$
0.6
0.4
0.2
0
-0.2
AB
0
s
$\frac{\sigma_y}{\sigma_o}$
2.4
2.2
1.8
1.6
1.4
1.2
1.0
0.8
0.6
0.4
0.2
O
A
B
1cm
$\frac{\tau_{xy}}{\tau_o}$
0.4
0.2
0
-0.2
-0.4

Fig. 6

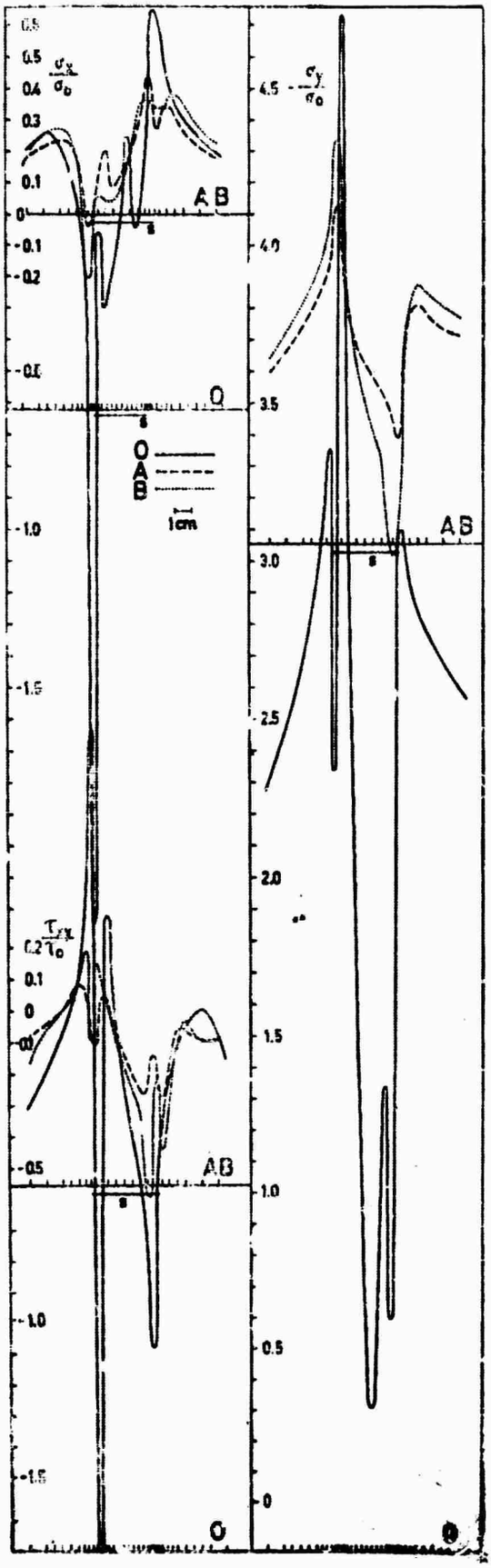

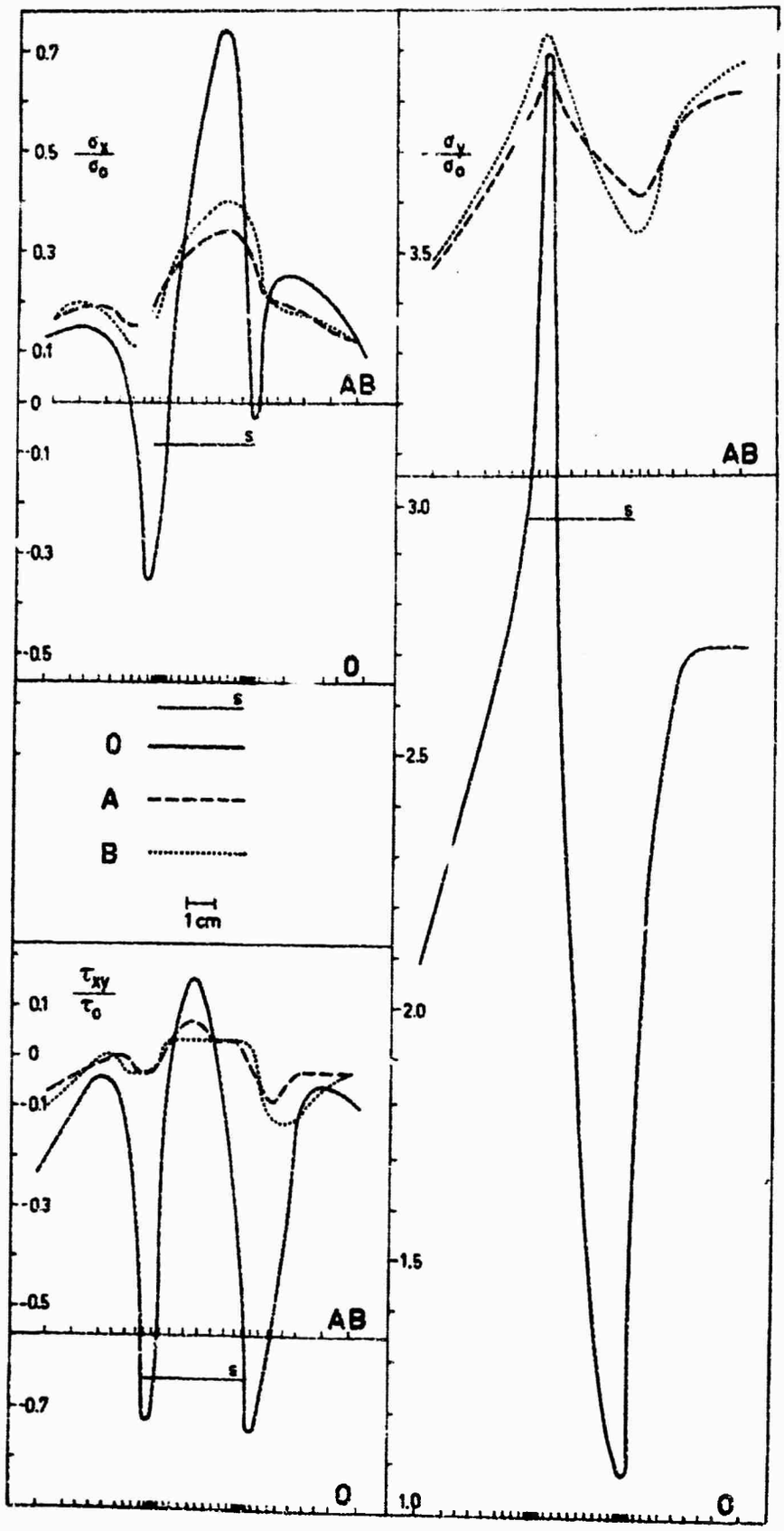
0.7
0.5
$\frac{\sigma_x}{\sigma_o}$
0.3
0.1
0
-0.1
-0.3
-0.5
AB
S
O
S
O
A
B
1 cm
$\frac{\tau_{xy}}{\tau_o}$
0.1
0
-0.1
-0.3
-0.5
AB
S
-0.7
O
$\frac{\sigma_y}{\sigma_o}$
3.5
AB
3.0
S
2.5
2.0
1.5
1.0
O

Fig. 8

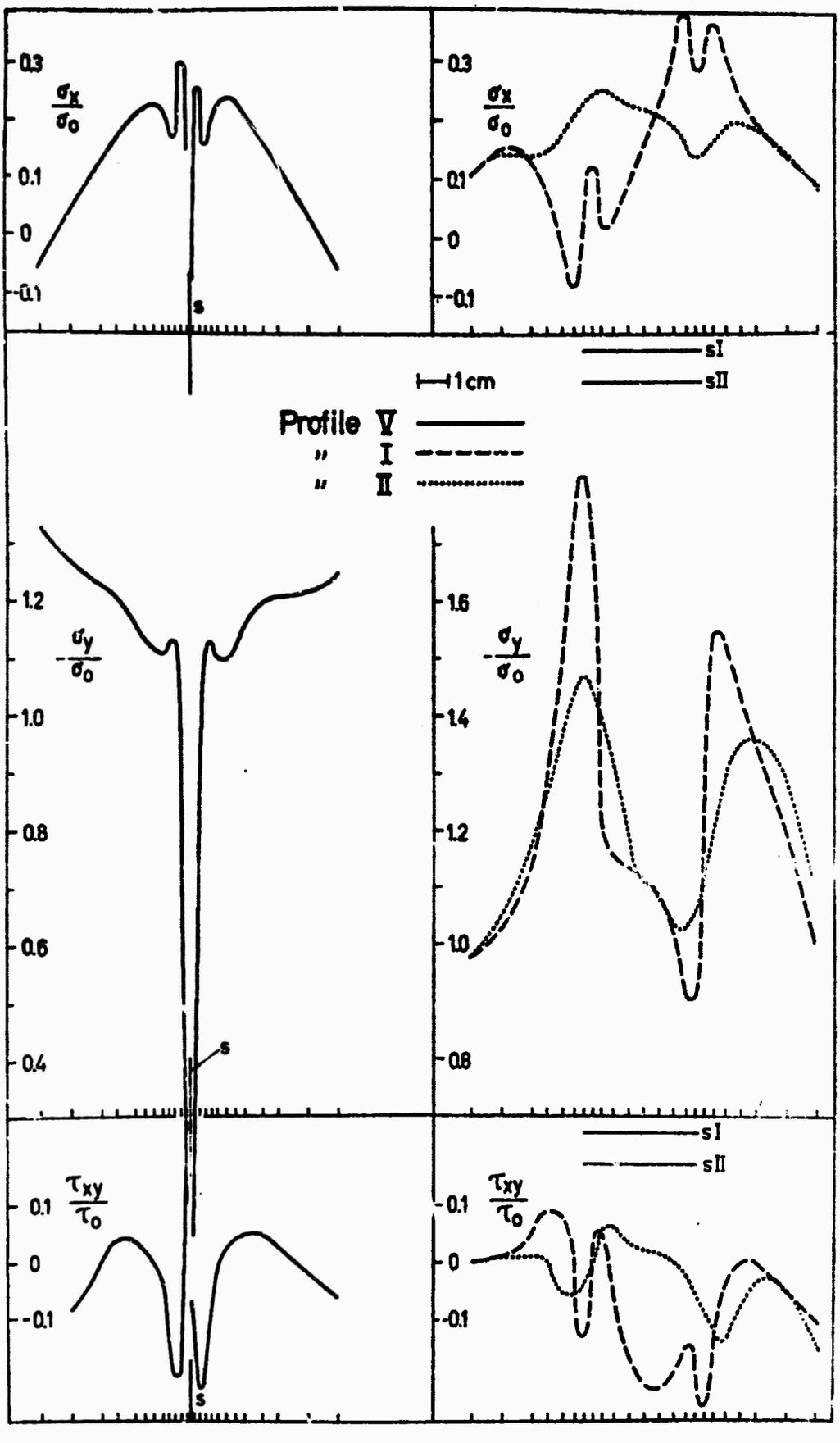
0.3
0.1
0
-0.1
$\frac{\sigma_x}{\sigma_0}$
s
sI
sII
1cm
Profile V
" I
" II
1.2
1.0
0.8
0.6
0.4
$\frac{\sigma_y}{\sigma_0}$
1.6
1.4
1.2
1.0
0.8
$\frac{\tau_{xy}}{\tau_0}$